



Two photon study of environmental effects on indole spectra  
by Aden Andrew Rehms

A thesis submitted in partial fulfillment of the requirements for the degree of Doctor of Philosophy in  
Chemistry

Montana State University

© Copyright by Aden Andrew Rehms (1990)

Abstract:

Polarized two-photon fluorescence excitation spectroscopy has been applied for the first time to the study of indole, the chromophore of the amino acid tryptophan. Investigations of three nine-membered ring systems, benzimidazole, benzimidazole cation, and indole have emphasized the utility of the experimental technique and revealed that the overlapping La and Lb states of indole have very different two-photon polarization ratios. Substituted indoles, with their varying La-Lb energy gaps, were studied in cyclohexane and n-butanol to explore the usefulness of the polarization ratio difference. The results of this study have directly confirmed the previously deduced La-Lb energy gaps in these compounds, the greater sensitivity of La to polar solvation, La-Lb level inversion, the role of La in producing broad red-shifted fluorescence, the existence of ground state complexes, and the importance of hydrogen bonding in the ground state complexes. The La Lb polarization ratio difference was also exploited to investigate the influence of charge on the La and Lb states. Experiments with tryptophan, 5-methoxytryptophan and yohimbine revealed the great sensitivity of the La state to a positive charge in the vicinity of the 5-ring of indole. The results with tryptophan also hint at a role of the Lb state in the dual exponential decay of tryptophan fluorescence. Two-photon spectra of all the aromatic amino acids and a comparison of the strength of their signals show tyrosine to be comparable to phenylalanine for two-photon excitation. Unlike the situation in one-photon spectroscopy, it may be possible to observe phenylalanine residues in proteins with two-photon spectroscopy. Finally, the first ever two-photon excitation spectrum of a small protein, melittin, shows that it is possible to observe a two-photon signal from a protein.

TWO PHOTON STUDY OF ENVIRONMENTAL  
EFFECTS ON INDOLE SPECTRA

by

Aden Andrew Rehms

A thesis submitted in partial fulfillment  
of the requirements for the degree

of

Doctor of Philosophy

in

Chemistry

MONTANA STATE UNIVERSITY  
Bozeman, Montana

February 1990

D378  
R2696

ii

APPROVAL

of a thesis submitted by

Aden Andrew Rehms

This thesis has been read by each member of the thesis committee and has been found to be satisfactory regarding content, English usage, format, citations, bibliographic style, and consistency, and is ready for submission to the College of Graduate Studies.

Feb 16, 1990

Date

Patrick R. Callis

Chairperson, Graduate Committee

Approved for the Major Department

January 13, 1990

Date

Edwin H. Abbott

Head, Major Department

Approved for the College of Graduate Studies

Feb 26, 1990

Date

Henry S. Parsons

Graduate Dean

## STATEMENT OF PERMISSION TO USE

In presenting this thesis in partial fulfillment of the requirements for a doctoral degree at Montana State University, I agree that the Library shall make it available to borrowers under rules of the Library. I further agree that copying of this thesis is allowable only for scholarly purposes, consistent with "fair use" as prescribed in the U.S. Copyright Law. Requests for extensive copying or reproduction of this thesis should be referred to University Microfilms International, 300 North Zeeb Road, Ann Arbor, Michigan 48106, to whom I have granted "the exclusive right to reproduce and distribute copies of the dissertation in and from microfilm and the right to reproduce and distribute by abstract in any format."

Signature

Robert A. Perkins

Date

1/8/90

## TABLE OF CONTENTS

	Page
INTRODUCTION . . . . .	1
EXPERIMENTAL . . . . .	4
Theory of Two-photon absorption . . . . .	4
Instrumentation and Procedures . . . . .	10
NINE-MEMBERED RING SYSTEMS: INDOLE AND BENZIMIDAZOLE . . . . .	17
Background . . . . .	17
Two-photon Spectra . . . . .	19
Discussion . . . . .	26
Indole . . . . .	26
Benzimidazole . . . . .	28
Benzimidazole Cation . . . . .	29
Summary . . . . .	30
SOLVENT AND SUBSTITUENT EFFECTS ON INDOLE . . . . .	31
Background . . . . .	31
Two-Photon Spectra . . . . .	35
Indoles in Cyclohexane . . . . .	35
5-methylindole (5MI) . . . . .	35
Indole . . . . .	35
1-methylindole (1MI) . . . . .	38
3-methylindole (3MI) . . . . .	38
2,3 dimethylindole (2,3MI) . . . . .	41
4-methoxyindole (4MI) . . . . .	43
5-methoxyindole (5MTI) . . . . .	43
6-methoxyindole (6MTI) . . . . .	46

TABLE OF CONTENTS -- Continued

	Page
7-methoxyindole (7MTI) . . . . .	48
Indoles in Butanol . . . . .	50
5-methylindole . . . . .	50
Indole . . . . .	50
1-methylindole . . . . .	55
3-methylindole . . . . .	55
2,3 dimethylindole . . . . .	55
4-methoxyindole . . . . .	55
5-methoxyindole . . . . .	64
6-methoxyindole . . . . .	64
7-methoxyindole . . . . .	64
Discussion . . . . .	64
Summary . . . . .	79
CHARGE EFFECTS . . . . .	81
Background . . . . .	81
Two-photon Spectra . . . . .	83
Discussion . . . . .	90
Summary . . . . .	97
AMINO ACIDS AND PROTEINS . . . . .	98
Background . . . . .	98
Two-photon Spectra . . . . .	99
Discussion . . . . .	105
Summary . . . . .	106

TABLE OF CONTENTS -- Continued

	Page
SUMMARY. . . . .	107
REFERENCES . . . . .	109

## LIST OF TABLES

Table	Page
1. INDO/s results for indoles studied. a) 10 x 20 singles only, Mataga-Nishimoto $\delta$ 's; b) 14 x 14 singles only Mataga-Nishimoto $\delta$ 's; c) 9 x 7 singles and doubles Ohno-Klopman $\delta$ 's . . . . .	27
2. Table of Results . . . . .	73

## LIST OF FIGURES

Figure	Page
1. Time-ordered Feynmann diagrams for a) A V coupling b) A A coupling and c) two consecutive A V couplings . . . . .	6
2. Laser apparatus utilized by the author to obtain the two-photon spectra in this study . .	12
3. Two-photon fluorescence excitation (solid line), one photon absorption (dashed line), and two-photon polarization (dotted line) spectra for indole dissolved in cyclohexane. (0.2M excitation, 0.05M polarization . . . . .	20
4. Two-photon fluorescence excitation (solid line), one photon absorption (dashed line), and two-photon polarization (dotted line) spectra for benzimidazole dissolved in isopropanol (0.2M) . . . . .	22
5. Two-photon fluorescence excitation (solid line), one photon absorption (dashed line), and two-photon polarization (dotted line) spectra for benzimidazole dissolved in methanol + H <sub>2</sub> SO <sub>4</sub> (0.2M) . . . . .	24
6. Relative two-photon absorptivities for indole, benzimidazole, benzimidazole cation, and toluene . . . . .	25
7. Indole ring numbering system . . . . .	31
8. Two-photon fluorescence excitation (solid line), one photon absorption (dashed line), and two-photon polarization (dotted line) spectra for 5-methylindole dissolved in cyclohexane (0.01M) . . . . .	36
9. Two-photon fluorescence excitation (solid line), one photon absorption (dashed line), and two-photon polarization (dotted line) spectra for indole dissolved in cyclohexane (0.01M) . . . . .	37

LIST OF FIGURES -- Continued

Figure	Page
10. Two-photon fluorescence excitation (solid line), one photon absorption (dashed line), and two-photon polarization (dotted line) spectra for 1-methylindole dissolved in cyclohexane (0.01M) . . . . .	39
11. Two-photon fluorescence excitation (solid line), one photon absorption (dashed line), and two-photon polarization (dotted line) spectra for 3-methylindole dissolved in cyclohexane (0.01M) . . . . .	40
12. Two-photon fluorescence excitation (solid line), one photon absorption (dashed line), and two-photon polarization (dotted line) spectra for 2,3-dimethylindole dissolved in cyclohexane (0.01M) . . . . .	42
13. Two-photon fluorescence excitation (solid line), one photon absorption (dashed line), and two-photon polarization (dotted line) spectra for 4-methoxyindole dissolved in cyclohexane (0.004M) . . . . .	44
14. Two-photon fluorescence excitation (solid line), one photon absorption (dashed line), and two-photon polarization (dotted line) spectra for 5-methoxyindole dissolved in cyclohexane (0.004M) . . . . .	45
15. Two-photon fluorescence excitation (solid line), one photon absorption (dashed line), and two-photon polarization (dotted line) spectra for 6-methoxyindole dissolved in cyclohexane (0.004M) . . . . .	47
16. Two-photon fluorescence excitation (solid line), one photon absorption (dashed line), and two-photon polarization (dotted line) spectra for 7-methoxyindole dissolved in cyclohexane (0.004M) . . . . .	49

LIST OF FIGURES -- Continued

Figure	Page
17. Two-photon fluorescence excitation (solid line), one photon absorption (dashed line), and two-photon polarization (dotted line) spectra for 5-methylindole dissolved in butanol (0.01M) . . . . .	51
18. Two-photon polarization spectra of 5-methylindole in cyclohexane (solid line) and in butanol (dotted line) (0.01M) . . . . .	52
19. One-photon absorption and fluorescence spectra of 5-methylindole in cyclohexane (solid lines) and in butanol (dotted lines) ( $\sim 10^{-5}M$ ) . . . . .	52
20. Two-photon fluorescence excitation (solid line), one photon absorption (dashed line), and two-photon polarization (dotted line) spectra for indole dissolved in butanol (0.01M) . . . . .	53
21. Two-photon polarization spectra of indole in cyclohexane (solid lines) and in butanol (dotted line) (0.01M) . . . . .	54
22. One-photon absorption and fluorescence spectra of indole in cyclohexane (solid lines) and in butanol (dotted line) (0.01M) . . . . .	54
23. Two-photon fluorescence excitation (solid line), one photon absorption (dashed line), and two-photon polarization (dotted line) spectra for 1-methylindole dissolved in butanol (0.01M) . . . . .	56
24. Two-photon polarization spectra of 1-methylindole in cyclohexane (solid line) and in butanol (dotted line) (0.01M) . . . . .	57
25. One-photon absorption and fluorescence spectra of 1-methylindole in cyclohexane (solid lines) and in butanol (dotted lines) ( $\sim 10^{-5}M$ ) . . . . .	57

LIST OF FIGURES -- Continued

Figure	Page
26. Two-photon fluorescence excitation (solid line), one photon absorption (dashed line), and two-photon polarization (dotted line) spectra for 3-methylindole dissolved in butanol (0.01M) . . . . .	58
27. Two-photon polarization spectra of 3-methylindole in cyclohexane (solid line) and in butanol (dotted line) (0.01M) . . . . .	59
28. One-photon absorption and fluorescence spectra of 3-methylindole in cyclohexane (solid lines) and in butanol (dotted lines) ( $\sim 10^{-5}M$ ) . . . . .	59
29. Two-photon fluorescence excitation (solid line), one photon absorption (dashed line), and two-photon polarization (dotted line) spectra for 2,3-dimethylindole dissolved in butanol (0.01M) . . . . .	60
30. Two-photon polarization spectra of 2,3-dimethylindole in cyclohexane (solid line) and in butanol (dotted line) (0.01M) . . . . .	61
31. One-photon absorption and fluorescence spectra of 2,3-dimethylindole in cyclohexane (solid lines) and in butanol (dotted lines) ( $\sim 10^{-5}M$ ) . . . . .	61
32. Two-photon fluorescence excitation (solid line), one photon absorption (dashed line), and two-photon polarization (dotted line) spectra for 4-methoxyindole dissolved in butanol (0.004M) . . . . .	62
33. Two-photon polarization spectra of 4-methoxyindole in cyclohexane (solid line) and in butanol (dotted line) (0.004M) . . . . .	63
34. One-photon absorption and fluorescence spectra of 4-methoxyindole in cyclohexane (solid lines) and in butanol (dotted lines) ( $\sim 10^{-5}M$ ) . . . . .	63

LIST OF FIGURES -- Continued

Figure	Page
35. Two-photon fluorescence excitation (solid line), one photon absorption (dashed line), and two-photon polarization (dotted line) spectra for 5-methoxyindole dissolved in butanol (0.004M) . . . . .	65
36. Two-photon polarization spectra of 5-methoxyindole in cyclohexane (solid line) and in butanol (dotted line) (0.004M) . . . . .	66
37. One-photon absorption and fluorescence spectra of 5-methoxyindole in cyclohexane (solid lines) and in butanol (dotted lines) (~10 <sup>-5</sup> M) . . . . .	66
38. Two-photon fluorescence excitation (solid line), one photon absorption (dashed line), and two-photon polarization (dotted line) spectra for 6-methoxyindole dissolved in butanol (0.004M) . . . . .	67
39. Two-photon polarization spectra of 6-methoxyindole in cyclohexane (solid line) and in butanol (dotted line) (0.004M) . . . . .	68
40. One-photon absorption and fluorescence spectra of 6-methoxyindole in cyclohexane (solid lines) and in butanol (dotted lines) (~10 <sup>-5</sup> M) . . . . .	68
41. Two-photon fluorescence excitation (solid line), one photon absorption (dashed line), and two-photon polarization (dotted line) spectra for 7-methoxyindole dissolved in butanol (0.004M) . . . . .	69
42. Two-photon polarization spectra of 7-methoxyindole in cyclohexane (solid line) and in butanol (dotted line) (0.004M) . . . . .	70
43. One-photon absorption and fluorescence spectra of 7-methoxyindole in cyclohexane (solid lines) and in butanol (dotted lines) (~10 <sup>-5</sup> M) . . . . .	70

LIST OF FIGURES -- Continued

Figure	Page
44. Comparison of the effect of polar solvation on the polarization spectra of indole and 1-methylindole. Indole in cyclohexane (dashed line) and in butanol (dash-dotted line). 1-methylindole in cyclohexane (solid line) and in butanol (dotted line) . . . . .	75
45. Comparison of the effect of polar solvation on the fluorescence spectra of indole (solid lines) and 1-methylindole (dotted lines). In each case the broad fluorescence is that seen in polar solvents . . . . .	78
46. Permanent dipole moments for the ground ( $\mu_g$ ), Lb ( $\mu_{Lb}$ ), and La ( $\mu_{La}$ ) states of indole . . . . .	82
47. Structure of Yohimbine . . . . .	82
48. Two-photon fluorescence excitation (solid line), one photon absorption (dashed line), and two-photon polarization (dotted line) spectra of Yohimbine dissolved in isopropanol at high pH ( $5 \times 10^{-3}M$ ) . . . . .	84
49. Two-photon fluorescence excitation (solid line), one photon absorption (dashed line), and two-photon polarization (dotted line) spectra of Yohimbine dissolved in isopropanol at low pH ( $5 \times 10^{-3}M$ ) . . . . .	85
50. Two-photon fluorescence excitation (solid line), one photon absorption (dashed line), and two-photon polarization (dotted line) spectra of 5-methoxytryptophan in pH 11 phosphate buffer (0.01M) . . . . .	87
51. Two-photon fluorescence excitation (solid line), one photon absorption (dashed line), and two-photon polarization (dotted line) spectra of 5-methoxytryptophan in pH 7 phosphate buffer (0.01M) . . . . .	88

LIST OF FIGURES -- Continued

Figure	Page
52. Two-photon fluorescence excitation (solid line), one photon absorption (dashed line), and two-photon polarization (dotted line) spectra of 5-methoxytryptophan in pH 2 phosphate buffer (0.01M) . . . . .	89
53. Two-photon fluorescence excitation (solid line), one photon absorption (dashed line), and two-photon polarization (dotted line) spectra of tryptophan in pH 11 phosphate buffer (0.01M) . . . . .	91
54. Two-photon fluorescence excitation (solid line), one photon absorption (dashed line), and two-photon polarization (dotted line) spectra of tryptophan in pH 7 phosphate buffer (0.01M) . . . . .	92
55. Two-photon fluorescence excitation (solid line), one photon absorption (dashed line), and two-photon polarization (dotted line) spectra of tryptophan in pH 2 phosphate buffer (0.01M) . . . . .	93
56. Comparison of the polarization spectra of tryptophan at pH 2 (solid line), pH 7 (dotted line) and pH 11 (dashed line) . . . . .	94
57. Two-photon fluorescence excitation (solid line), one photon absorption (dashed line), and two-photon polarization (dotted line) spectra of phenylalanine in pH7 buffer (0.01M) . . . . .	100
58. Two-photon fluorescence excitation (solid line), one photon absorption (dashed line), and two-photon polarization (dotted line) spectra of tyrosinamide in pH 7 buffer . . . . .	101
59. Two-photon fluorescence excitation (solid line), one photon absorption (dashed line), and two-photon polarization (dotted line) spectra of tryptophan in pH 7 buffer . . . . .	102

LIST OF FIGURES -- Continued

Figure	Page
60. Relative signal from typtophan (solid line), tyrosinamide (dashed line), and phenylalanine (dotted line) measured at their respective fluorecence maxima . . . . .	103
61. Two-photon fluorecence excitation (solid line) and two-photon polarization spectra for the monomeric (dotted line) and tetrameric (dashed line) forms . . . . .	104

## ABSTRACT

Polarized two-photon fluorescence excitation spectroscopy has been applied for the first time to the study of indole, the chromophore of the amino acid tryptophan. Investigations of three nine-membered ring systems, benzimidazole, benzimidazole cation, and indole have emphasized the utility of the experimental technique and revealed that the overlapping  $L_a$  and  $L_b$  states of indole have very different two-photon polarization ratios. Substituted indoles, with their varying  $L_a$ - $L_b$  energy gaps, were studied in cyclohexane and n-butanol to explore the usefulness of the polarization ratio difference. The results of this study have directly confirmed the previously deduced  $L_a$ - $L_b$  energy gaps in these compounds, the greater sensitivity of  $L_a$  to polar solvation,  $L_a$ - $L_b$  level inversion, the role of  $L_a$  in producing broad red-shifted fluorescence, the existence of ground state complexes, and the importance of hydrogen bonding in the ground state complexes. The  $L_a$ - $L_b$  polarization ratio difference was also exploited to investigate the influence of charge on the  $L_a$  and  $L_b$  states. Experiments with tryptophan, 5-methoxytryptophan and yohimbine revealed the great sensitivity of the  $L_a$  state to a positive charge in the vicinity of the 5-ring of indole. The results with tryptophan also hint at a role of the  $L_b$  state in the dual exponential decay of tryptophan fluorescence. Two-photon spectra of all the aromatic amino acids and a comparison of the strength of their signals show tyrosine to be comparable to phenylalanine for two-photon excitation. Unlike the situation in one-photon spectroscopy, it may be possible to observe phenylalanine residues in proteins with two-photon spectroscopy. Finally, the first ever two-photon excitation spectrum of a small protein, melittin, shows that it is possible to observe a two-photon signal from a protein.

## INTRODUCTION

The near ultraviolet absorption and fluorescence of proteins can be ascribed to the aromatic amino acids phenylalanine, tyrosine, and tryptophan (1). Absorption and emission of light by these amino acids have been exploited to study protein structure and dynamics (2,3,4,). The most useful of these is tryptophan, whose indole chromophore is highly sensitive to local solvation and structural environment. The lowest energy UV absorption band of indole consists of two nearly degenerate electronic transitions designated  $L_a$  and  $L_b$  (5). One photon studies have indicated that solvent(6,7,8,9,10), substitution (7,8,9), and charge (11) can differentially shift the  $L_a$  and  $L_b$  states and lead to large changes in the fluorescence spectra of indoles. This occurs without great alterations to their absorption spectra (12,13,14,15).

Perhaps the most notable characteristic of indole photophysics is the large stokes shift of the fluorescence in polar media. Red shifts of the fluorescence relative to that seen in hydrocarbon solvents occur for additions of polar solvent insufficient to alter the bulk dielectric properties of the solvent. Accompanying the red shift is a loss of structure in the fluorescence. It appears that polar solvents interact with indoles in a specific manner (12,13,14). Solvents also seem to have more general effects

on the fluorescence (15,16,17,18,19). The hypotheses advanced to explain how the solvent causes the large red shift of indole fluorescence are based upon solvent shift studies of absorption and fluorescence peaks.

Unfortunately, the broad nature of the transitions and complications due to dual absorption and emission from the  $L_a$  and  $L_b$  states make such studies subject to errors. What has been needed to resolve some of these questions is a way of separating the contribution of each state to these processes. Polarized fluorescence excitation has been used to resolve the band shapes of  $L_a$  and  $L_b$  in polar solvents (20,21) but has failed in hydrocarbon solvents where minute amounts of polar impurities complex with indoles at the low temperatures necessary to perform the experiments (22). Substituent perturbation (9,23) and derivative spectroscopy (24) have also been tried with largely unsatisfactory results.

Polarized two-photon fluorescence excitation offers a direct method of observing the  $L_a$  and  $L_b$  states separately in absorption. This technique involves the essentially simultaneous absorption of visible photons to reach excited states of ultraviolet energies. The simultaneous nature of the absorption makes it possible to observe a polarization dependence from non-rigid samples. It was discovered as part of this thesis work (25) that the  $L_a$  and  $L_b$  states of indole are characterized by very different two-photon

polarization ratios. This enabled the author to directly observe regions of  $L_a$  and  $L_b$  absorption.

The aim of this thesis was to utilize this powerful technique to learn more about the relative response of  $L_a$  and  $L_b$  to solvent, substitution, and charge. Indole and various of its methyl and methoxy derivatives were examined in hydrocarbon and alcohol solvents. Models for charge interactions, which included the amino acid tryptophan itself, were also examined. These two-photon experiments represent the first time this technique has been used to look at indoles and were designed to answer specific questions about the validity of conclusions drawn from the indirect one photon methods used by others. The results for these models systems combined with two-photon spectra of all the aromatic amino acids and a small protein, melittin, serve to pave the way for two-photon spectroscopy of proteins. INDO/S calculations have been compared to the experimental results to test their predictions so that they might also prove useful for interpretation of indole and protein spectra.

**EXPERIMENTAL**Theory of Two-photon absorption

The simultaneous absorption of two non-resonant photons by matter was first postulated to occur by Maria Goeppert-Mayer in 1931 (26). Observation of this phenomenon at optical frequencies had to await the advent of the laser (27) because of the inherently low transition probabilities associated with two-photon processes. Once practical, this new spectroscopy offered many unique possibilities and was quickly utilized to investigate a large number of compounds (28,29). Theoretical advances (30-40) of the period allowed experiments to be designed and gave a deeper insight into the regularities emerging in two-photon spectra of aromatic molecules.

Second order time-dependent perturbation theory predicts that molecules can absorb two photons through two types of interaction with the radiation. The relativistically invariant form of the Hamiltonian for a system in the presence of an electromagnetic field is given by (41)

$$H = \frac{1}{2m} \left( p - \frac{e}{c} A \right)^2 + [V(r) + e\phi]$$

where  $A$  is the vector potential of the radiation field given by

$$A(r,t) = A_0 \cos(\omega t - k \cdot r)$$

$\phi$  is the scalar potential associated with the electromagnetic field, and  $V(r)$  is an effective potential for a given electron due to the nuclei and other electrons in the system. Writing all the terms of equation 1 in detail, the Hamiltonian is

$$H = \frac{1}{2m} (-\hbar^2 \nabla^2 + i\hbar \frac{e}{c} \mathbf{A} \cdot \nabla + \frac{e^2}{c^2} |\mathbf{A}|^2) + V(r) + e\phi$$

If the coulomb gauge is chosen, it provides that  $\nabla \cdot \mathbf{A} = 0$  and  $\phi = 0$ . The equation above becomes

$$H = \frac{1}{2m} (-\hbar^2 \nabla^2 + 2i\hbar \frac{e}{c} \mathbf{A} \cdot \nabla + \frac{e^2}{c^2} |\mathbf{A}|^2) + V(r)$$

Rewriting this as

$$H = H^0 + H' = \left[ -\frac{\hbar^2}{2m} \nabla^2 + V(r) \right] + \left[ \frac{ie\hbar}{mc} \mathbf{A} \cdot \nabla + \frac{e^2}{2mc^2} |\mathbf{A}|^2 \right]$$

it is clear that the perturbation is

$$H' = \frac{ie\hbar}{mc} \mathbf{A} \cdot \nabla + \frac{e^2}{2mc^2} |\mathbf{A}|^2$$

These two terms describe the coupling with the electromagnetic field that lead to changes in the state function of the system. In Figure 1 are the time ordered Feynmann (42) diagrams which correspond to the couplings described by the  $\mathbf{A} \cdot \nabla$  and  $\mathbf{A} \cdot \mathbf{A}$  terms. The straight upward arrows represent a molecule moving through time and space in state  $\psi^0$  and the wiggly arrows are photons which may interact with the molecule and leave the molecule in a state  $\psi_{\pm}$ . Since the  $\mathbf{A} \cdot \mathbf{A}$  term involves 2 photons it makes no contribution to ordinary one photon processes. The calculations of McClain and Harris (31), Honig et al.

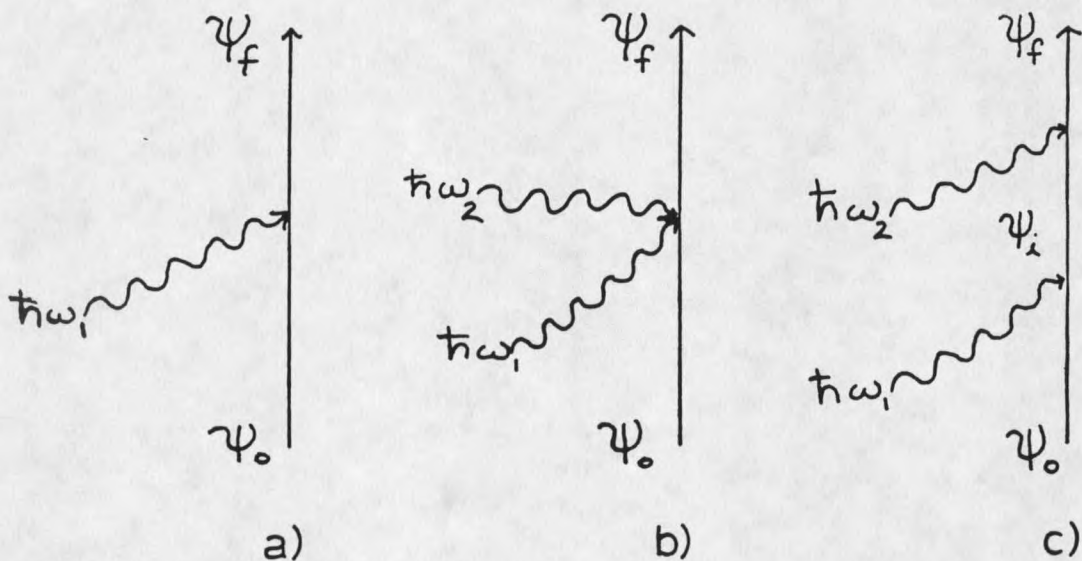


Figure 1: Time-ordered Feynmann diagrams for a)  $A \cdot \nabla$  coupling b)  $A \cdot A$  coupling and c) two consecutive  $A \cdot \nabla$  couplings.

(32,33), and Guccione and Van Kranendonk (43) have indicated that even for two photon absorption, the  $A \cdot A$  term gives little contribution. The Hamiltonian can now be taken as

$$H^0 = H^0 + H' = \left[ \frac{-\hbar^2}{2m} \nabla^2 + V(r) \right] + \frac{ie\hbar}{mc} A \cdot \nabla$$

With the appropriate Hamiltonian it is possible to proceed with a time-dependent perturbation treatment to arrive at the perturbed wavefunction in second order.

$$\psi_0^{(2)}(r,t) = \psi_0^{(1)}(r,t) + \frac{q^2 \nabla^2 \omega^2}{\hbar^2} \frac{\Sigma}{f} S_{\sigma \neq \mu} \mu_r^{\sigma}(r) \left( \frac{1 - \exp[-i(\omega_{\neq \sigma} - 2\omega)]}{\omega_{\neq \sigma} - 2\omega} \right)$$

Like one-photon processes, the transition rate for the two-photon process is proportional to the square of the coefficient of the final state  $\mu_r^{\sigma}$ . It is (31)

$$W_{g \neq f}^{(2)} = 128\pi^3 \alpha^2 \omega^2 F^2 |S_{g \neq f}|^2 g_m(2\omega)$$

This equation demonstrates the quadratic dependence of the transition rate on the photon flux (F) which distinguishes two-photon from one-photon processes. Dividing out the flux gives a purely molecular quantity,  $\delta_{g \neq f}$ , the two-photon absorptivity, given by (31)

$$\delta_{g \neq f} = 128\pi^3 \alpha^2 |S_{g \neq f}|^2 g_m(2\omega)$$

In both cases above  $S_{g \neq f}$  (assuming 2 identical photons) is (31)

$$S_{g \neq f} = \frac{\sum (e \cdot \langle f | r | k \rangle) (\langle k | r | g \rangle \cdot e)}{k \omega_{kg} - \omega}$$

$S_{g \neq f}$ , the two-photon tensor, demonstrates the complementary nature of one and two-photon processes. The dipole moment operator appears twice in  $S_{g \neq f}$  and both transitions  $k \leftarrow g$  and  $f \leftarrow k$  must be parity allowed (i.e. one-photon allowed) for the two-photon transition to be allowed. For gerade ground states this corresponds to successive  $u \leftarrow g$  and  $g \leftarrow u$  transitions for an overall  $g \leftarrow g$  parity selection rule. The Feynmann diagram, which corresponds to the two successive  $A \cdot V$  couplings suggested by the two-photon tensor, is also shown in Figure 1.

The states  $|k\rangle$  over which the tensor is summed are termed intermediate states and should include the initial and final states (35,39,40). Inclusion of the ground and final states is especially important in the description of polar molecules, where there are states characterized by

large changes in permanent dipole moment (39). This can be seen by looking only at the two terms in the sum over intermediate states which correspond to the ground and final states as intermediate states. The two terms are:

$$S = \frac{\langle f|r|g\rangle\langle g|r|g\rangle}{\omega_{gg}-\omega} + \frac{\langle f|r|f\rangle\langle f|r|g\rangle}{\omega_{fg}-\omega}$$

If the matrix elements of the dipole operator are denoted in the form  $R_{xy}$  this can be written as

$$S_{\text{partial}} = \frac{R_{fg} R_{gg}}{\omega_{gg}-\omega} + \frac{R_{ff} R_{fg}}{\omega_{fg}-\omega}$$

Recognizing that  $\omega_{gg} = 0$  and  $\omega_{fg} = 2\omega$  for identical photons

$$S_{\text{partial}} = \frac{R_{fg} R_{gg}}{-\omega} + \frac{R_{ff} R_{fg}}{\omega}$$

which leads to

$$S_{\text{partial}} = \frac{R_{fg}}{\omega} (R_{ff} - R_{gg})$$

$R_{fg}$  is simply the matrix element of a one-photon (dipole induced) transition from the ground state to the final state and  $(R_{ff} - R_{gg})$  is the difference in the permanent dipole moment of final and ground states. Thus, for the ground and final states to be important as intermediate states, the transition must be one-photon allowed and there must be a considerable change in permanent dipole moment between the ground and final states. Such an addition to  $S_{gf}$  is not important for centrosymmetric molecules, but is for polar molecules like the indoles studied in this thesis. If the transition dipole and the change in dipole moment are collinear, an additional contribution to  $\delta_{gf}$  proportional to

the oscillator strength of the transition  $f \leftarrow g$  and the square of the change in dipole moment given in debyes is introduced. The contribution of dipole terms for equally polarized photons of the same energy in the case where  $R_{fg}$  is parallel to  $R_{ff} - R_{gg}$  is in gm given by (39)

$$\delta_{\uparrow\uparrow} = 1.043 \frac{f(\Delta\mu)^2}{\Delta E}$$

where  $f$  is the oscillator strength of  $f \leftarrow g$ ,  $\Delta\mu$  is the change in dipole moment (in debyes), and  $\Delta E$  is the excitation energy in eV. Excitation energies of 5eV associated with strong one-photon transitions ( $f=1$ ) and changes of dipole moment on the order of 2 debyes will produce extra two-photon absorptivity contributions as strong as a moderately intense two-photon transition (i.e., 1 Göppert-Mayer,  $1 \text{ gm} = 1 \times 10^{-50} \text{ cm}^2 \text{ sec}/\text{photon molecule}$ ).

The 3 x 3 cartesian tensorial nature of the two-photon process leads to a polarization dependence of  $\delta$  upon the light which survives averaging over all molecular orientations. This is not true for one-photon processes where the cross-section has no polarization dependence. The quantities which survive the orientation averaging are denoted  $\epsilon_f$ ,  $\epsilon_g$ , and  $\epsilon_h$  are defined as: (28)

$$\delta_f = S_{\alpha\alpha} S_{\beta\beta}^* = \sum_1^3 |\text{diagonal elements}|^2$$

$$\delta_g = S_{\alpha\beta} S_{\alpha\beta} = \sum_1^3 |\text{each element}|^2$$

$$\delta_h = S_{\alpha\beta} S_{\beta\alpha} = \sum_1^3 |\text{hermitian products}|$$

Identical photons from the same laser beam make  $\delta_g = \delta_h$ . Information about the elements of the tensor can still be obtained from the relation for the absorptivity of circularly versus linearly polarized light. This quantity,  $\Omega$ , the two-photon polarization ratio, is defined as (37)

$$\Omega = \frac{\delta_{\text{cir}}}{\delta_{\text{lin}}} = \frac{\delta_x + 3\delta_y}{\delta_x + 2\delta_y}$$

Upper and lower limits on the value of  $\Omega$  are exhibited by tensors with the following patterns of elements.

$$\begin{pmatrix} 0 & 1 & 1 \\ 1 & 0 & 1 \\ 1 & 1 & 0 \end{pmatrix}$$

$$\Omega = 3/2$$

$$\begin{pmatrix} 1 & 0 & 0 \\ 0 & 1 & 0 \\ 0 & 0 & 1 \end{pmatrix}$$

$$\Omega = 0$$

The value of  $\Omega$  will in general be different for every transition. Molecules which are symmetric will exhibit characteristic tensor patterns for each symmetry species. In order to assign a polarization ratio to a given state for molecules which lack symmetry it is necessary to rely upon approximate molecular orbital calculations such as CNDO/S and INDO/S (35,36,38).

### Instrumentation and Procedures

The two-photon fluorescence excitation spectra recorded in this study were obtained using the apparatus drawn schematically in Figure 2. The spectra of benzimidazole,

benzimidazole cation, and indole in cyclohexane were taken with an NRG 0.5 MW (peak) nitrogen pump laser and an NRG single stage scanning dye laser as the light source. Early work on the methylindoles (44) also utilized this laser system. Subsequent spectra of the methylindoles and the spectra of all other molecules were obtained using a Lumonics HD 300 dye laser (8ns, <13mJ/pulse) pumped by the 2nd or 3rd Harmonic of a JK HY200 Nd:YAG laser. A Gallilean telescope expanded and collimated the dye laser beam. It was then routed through a shutter to the glan polarizer which polarized it vertically. A double fresnel rhombahedron on a rotating mount served to rotate the plane of polarization 45° before the beam passed through a stationary fresnel rhombahedron. Linearly and circularly polarized light utilized for measuring  $\Omega$  were produced here. The shutter and the double rhomb were both rotated by stepping motors under computer control. The beam was either left unfocused or focused slightly from 8 mm in diameter to 4-6 mm in diameter, depending upon the dye being utilized and the sample characteristics. In all cases the peak power density at the sample was below  $1.25 \times 10^{10} \text{ Wm}^{-2}$ . The signal from the sample was also checked for quadratic behavior by attenuating the beam with crossed polarizers. If the quadratic condition was met, a reduction of the laser energy by 50% led to a two-photon excited fluorescence signal of

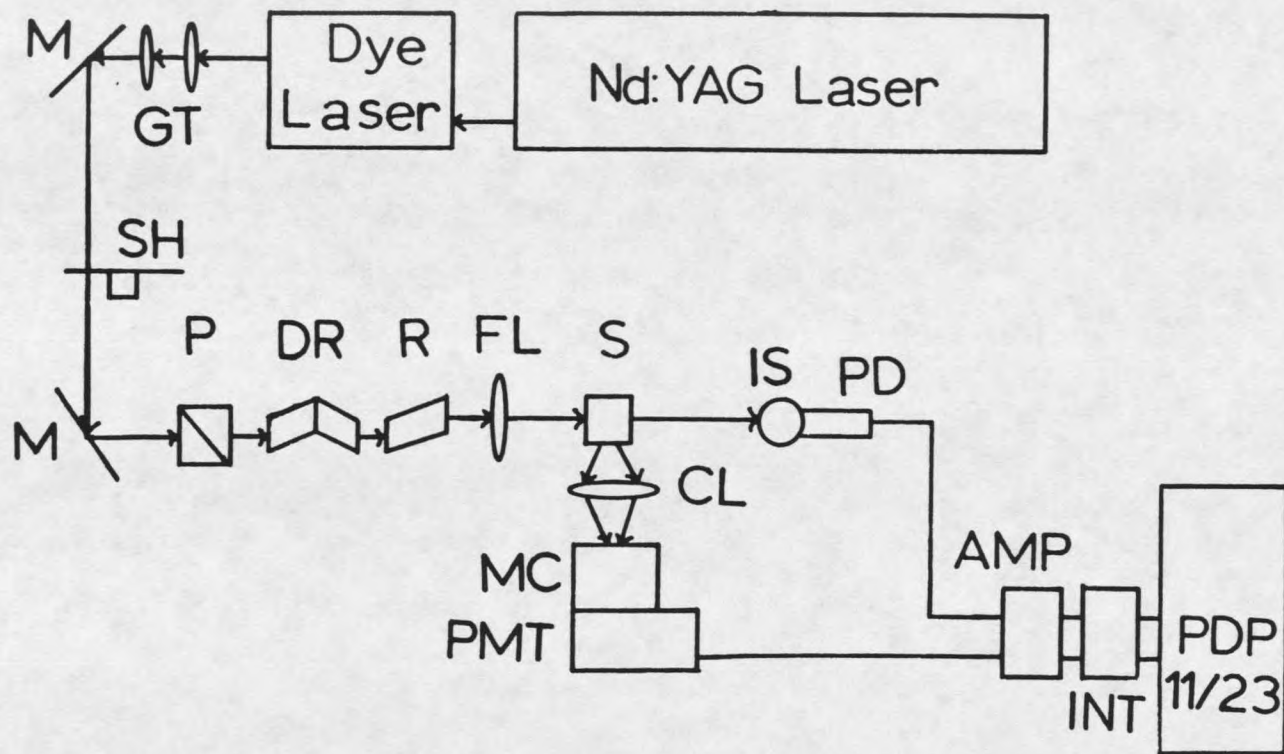


Figure 2: Laser apparatus utilized by the author to obtain the two-photon spectra in this study. GT (gallilean telescope), M (mirror), SH (shutter), P (glan polarizer), DR (double fresnel rhomb), R (fresnel rhomb), FL (focussing lens), S (sample), IS (integrating sphere), PD (photodiode), CL (cylindrical lens), MC (monochromator), PMT (photomultiplier tube), AMP (amplifier), INT (integrator).

25% of the original. These checks were performed at both ends of the dye ranges, the maxima of the dye gain curves, and at peaks due to molecular transitions. Defocusing was performed if necessary. The fluorescence of the sample was collected at right angles by an f3.0 quartz cylindrical lens, which focused it through 2 UV-pass filters (Schott UG-11) and onto the slit of an f/3.3 holographic grating monochromator (Instruments SA, 50 nm bandpass, 16 nm for early work where polarizer was rotated). No slits were used because slight changes in beam height due to the rotation of the double rhomb moved the beam off of the slit, giving a low reading for the circular signal. The laser beam was passed through the sample and into an integrating sphere where a quantum counting solution and a photodiode generated a signal proportional to the average photon flux. Below 600 nm Rhodamine (3g/l) was used as the quantum counter and above 600 nm, Nile Blue (1g/l). The fluorescence signal and the reference signal were amplified and integrated (200  $\mu$ s) using printed circuit boards purchased from Evans Associates. Integrated signals were stored and processed by a PDP 11/23 computer which also controls the stepping motors and the laser scan control unit. In a typical experiment the signals from the sample fluorescence and the laser reference detectors were averaged for 400 shots. The average of the sample signal was then divided by the square of the reference signal to obtain the normalized two-photon

signal. This was done at each wavelength using linearly polarized light to measure the two-photon fluorescence excitation spectrum. Determinations of the two-photon polarization ratio ( $\Omega$ ) were made at each wavelength using circularly polarized light for excitation and dividing the resulting two-photon signal by that just obtained for linearly polarized excitation.

Nine organic dyes and mixtures thereof covering a wavelength range of 440 nm to 650 nm were utilized in the dye laser to obtain the data segments. At least 5 nm of overlap was maintained between dye segments and they were joined to create the two-photon spectra. A more exact method of joining these segments to create a complete two-photon excitation spectrum has been developed recently by Jones and Callis (45). Within the range of 600 nm to 650 nm, this SHG technique was used as published. It involves second harmonic generation (SHG) from a powder sample of potassium di-hydrogen phosphate (KDP) to obtain a reference signal proportional to the instantaneous photon flux squared. The signal is used to compensate for changes in the temporal and spatial profiles of the laser beam to which the one photon reference is insensitive. In an attempt to extend the technique to shorter wavelengths, suspensions of urea crystals (75-150  $\mu\text{m}$ ) in decalin were tried. A quantum counting solution of 1g/l skatole in n-butanol was also added to remove the strong wavelength dependence below

600 nm of the UV pass filters used to separate the second harmonic from the fundamental. These efforts were successful in extending the technique with reasonable confidence to 530 nm where absorption by the decalin and possible scattering due to the mismatch of the refractive indices of decalin and urea caused the corrected two-photon signal to increase. Where reliable SHG data was obtained the procedure was utilized. All segments, corrected or not, were joined at the middle of the overlap and truncated so as to maintain the shape indicated by the midsection of each segment.

All solutes and solvents were of the highest quality available and used as received. Solutions were checked with 1-photon fluorescence excitation (Spex Fluorolog) and revealed no interfering fluorescent impurities. All solutions were approximately 0.01M except as indicated. Absorption spectra of dilute ( $10^{-5}$  M) solutions were obtained with a Cary 14 spectrophotometer. Fluorescence spectra were taken with the Spex Fluorolog.

Relative two-photon absorptivities ( $\delta$ ) for the benzimidazoles, toluene, and indole were determined by measuring the relative fluorescence signal excited by one and two-photon absorption. A 150 W Xenon arc lamp and a 0.5M grating monochromator were used for UV excitation. The detection geometry for both one and two-photon excitation

was kept constant. The relative two-photon absorptivity was then calculated from the relation

$$S_A^{(2)}/S_B^{(2)} = \epsilon_A C_A \phi_A(\lambda_A) / \epsilon_B C_B \phi_B(\lambda_B)$$

where  $S^{(2)}$  is the photon flux normalized two-photon signal for sample A,  $C_A$  its concentration, and  $\phi_A(\lambda_A)$  its differential fluorescence quantum yield.  $\phi$  represents the probability an absorbed photon will be emitted between wavelength  $\lambda$  and  $\lambda+d\lambda$ . The assumption of  $S_A^{(2)} = G\phi_A(\lambda_A)$  where  $G$  is the combined instrumental response function allowed calculation of  $\delta_s$ . Underlying the whole procedure is the assumption that the quantum yield per excitation is the same for one and two-photon excitation.

Molecular orbital calculations of one and two-photon properties were performed using a spectroscopically calibrated INDO/S program originally obtained from Dr. Michael Zerner, University of Florida(46), coupled to programs for calculating transition densities and two-photon properties.(47,48) Mataga-Nishimoto and Ohno-Klopman electron repulsion integrals were used for singly and doubly excited configuration calculations respectively.

**NINE-MEMBERED RING SYSTEMS: INDOLE AND BENZIMIDAZOLE**Background

Nine-membered heterocyclic aromatic ring systems are important in nature. They are found as the side chain of the amino acid tryptophan and are the basis for the nucleic acids adenine and guanine. These systems are non-alternate and lack symmetry, making it necessary to rely mostly upon semi-empirical molecular orbital calculations for theoretical insight. (48,49,50) The two lowest singlet  $\pi^* \leftarrow \pi$  states for indole have been assigned (1)  $L_B$  ( $S_1$ ) and  $L_a$  ( $S_2$ ) where the operational difference between the two states is that  $L_B$  is structured while  $L_a$  is broad and unstructured. This assignment appears to have followed the perimeter model classification scheme introduced by Platt. (5) While the  $L_a$  and  $L_B$  labels are meaningless for the odd-atom perimeter, a similarity exists between the transition density pattern (48) of the nine-ring states and the  $L_a$  and  $L_B$  states of benzene. Evleth (49) has also noted a similarity in the configuration wave functions.

The parent molecule for the nine-membered 10 pi electron series is the cyclononatetraenide anion. In this molecule the  $L_a$  and  $L_B$  states are degenerate. Callis (48) has discussed how cross-linking to form the 5-6 fused ring system of the indenyl anion ( $C_9H_7^{1-}$ ) removes this degeneracy. The  $L_a$  state appears to be mixed with the  $B_a$  state due to a

large  $L_a$ - $B_a$  transition density between the atoms that are cross-linked. The result is that the  $L_a$  state is greatly shifted to the red of the  $L_b$  state. Introduction of the nitrogen to form indole results in a cancellation of the effect of the cross-link and shifts the  $L_a$  state to the blue so that the two states are nearly degenerate again but with the  $L_b$  state now lowest. Introduction of another nitrogen at the 3 position to make benzimidole further shifts the  $L_a$  to the blue, separating them again. The inductive effect of the nitrogen has been discussed by Feitelson(50) as arising mainly from differences in the electrical charge distribution between the ground and excited states at the site of the nitrogen atom and he stressed the importance of including the interaction between the ground and excited states in the description of heteroatomic indene derivatives. He reasoned that since the inductive effect shifted the  $L_a$  and  $L_b$  states in different directions to leave  $L_b$  lowest for indole, electron donating groups at the 1 or 3 positions would lessen the inductive effect and lead to less of a blue shift for the  $L_a$  state. Indeed, the broad  $L_a$  state has been shown to move closer to the  $L_b$  state for tryptophan (3-substitution) (6) The importance of the charge density of the nitrogen can also be seen in Evleth's(49) work where moderate changes in the nitrogen parameters, leading to less of an inductive effect actually caused the  $L_a$  state to again become lowest for indole.

Since two-photon spectroscopy offers information complementary to that obtained with conventional one-photon spectroscopies, two-photon fluorescence excitation spectra of indole, benzimidazole, and benzimidazole cation were obtained. These experimental results have been used to judge the validity of INDO/S calculations. In order to further test the theory, measurements of relative two-photon absorptivities were made.

### Two-photon Spectra

Shown in Figure 3 are the two-photon fluorescence excitation for linearly polarized light (solid line), one-photon absorption (dashed lines), and two-photon polarization ratio (dotted lines) spectra for indole (0.2M). As is done throughout this thesis, the one-photon absorption is shifted from its one-photon wavelengths to correspond to wavelengths for two-photon absorption of the same total energy. The 0-0 of the absorption spectrum is also normalized to follow the 0-0 peak of the two-photon spectrum. The polarization spectrum shown is that obtained for a 0.05M solution.  $\Omega$  is seen to be near the theoretical maximum for the 0-0  $L_b$ . It then drops steeply, presumably due to the onset of  $L_a$  absorption, and levels off at  $\sim 0.7$ . The slight drop of the polarization ratio on the red edge is





























































































































































































